COMPUTERS AND BIOMEDICAL RESEARCH 17, 436–470 (1984)

A Model of the Mechanics of Binocular Alignment

JOEL M. MILLER* AND DAVID A. ROBINSON

Smith–Kettlewell Institute of Visual Sciences, Medical Research Institute, 2232 Webster Street, San Francisco, California 94115, and Wilmer Institute, The Johns Hopkins School of Medicine, Baltimore, Maryland 21205

Received January 24, 1984

A computer model (SQUINT) of the static mechanics of human eyes is developed and applied to the diagnosis and treatment of defects of binocular alignment (strabismus). Brief discussions of ocular anatomy, binocular vision, strabismus and its surgical correction, and early strabismus modeling are provided for nonspecialists in these areas. Models of muscle force, muscle path, globe translation, and binocularity are developed. To illustrate the use of the model in clinical cases, it is applied to the diagnosis and surgical treatment of a case of superior oblique palsy. The model's implementation under the UNIX operating system is described.

For vision to be normal, movements of the two eyes must be precisely coordinated over an adequate range. A diverse group of disorders, called *strabismus,* are characterized by failure of binocular coordination and, in some cases, by an abnormal range of movement. The result is that in at least some positions of gaze the two eyes fix different points in space.

We will be describing a model of the eyes' mechanics, oriented to simulate normal binocular coordination, strabismic misalignments of various kinds, eye muscle surgery, and certain other related procedures. To provide some necessary background we will begin by briefly discussing the anatomy of the eye, muscles and orbit, the dependence of binocular vision on binocular alignment, and the nature and treatment of strabismus. Next, we briefly summarize an early strabismus model introduced by Robinson (*1*). Then, the new model is described, after which we discuss some applications and tests. A final section describes the model's implementation under the UNIX[1] operating system.

1. THE EYE, MUSCLES, AND ORBIT

When we *fix* or look at some object in space, two related things occur: (1) The eyes rotate so that the fovea of each is brought to the position of the image formed by the eye's optics, and (2) the power of each lens is adjusted to bring the image into sharp focus (*accommodation*). Our interest is in fixation of

* Correspondence to Dr. Miller at the Smith–Kettlewell Institute.

[1] UNIX is a trademark of Bell Labs.

0010-4809/84 $3.00

targets in a frontal plane and in the misalignments which might occur over such a field; such fixation is accomplished by *conjugate* eye movements, in which the two eyes rotate in the same direction (say, to the right and up) and through (roughly) equal angles.

In our development we use the three coordinate systems shown in Fig. 1. The first, denoted xyz (Fig. 1A) is, for the left eye, a simple left-handed Cartesian system, fixed in the head: The positive x axis points laterally, the y axis forward (defining the straight-ahead or *primary* position) and the z axis up. The xyz axes are useful for the geometrical development, but are awkward for describing positions of the eye. To see this, consider an eye in primary position; upward rotation is conveniently described as rotation about the x axis. However, now consider an eye looking to one side; rotation about the x axis no longer moves it only up but also rolls it on its side. The Fick coordinate system, denoted $x'y'z'$ (Figs. 1B–E), moves with the eye and is better suited for describing eye movements. The angle ϑ (sometimes called *longitude*) is taken as *horizontal eye position*, and φ (*latitude*) as *vertical eye position*. The angle ψ by which the eye is rotated about y' is the *torsional eye position*. (The order of these rotations must, of course, be as described.) Positive directions of ϑ, φ, and ψ are indicated in Fig. 1B. Rotation in the positive ϑ or *temporal* direction is called *abduction* and rotation in the negative ϑ or *nasal* direction, *adduction*; positive φ is *elevation* which is opposite to *depression*; positive ψ is *extorsion*, opposite to *intorsion*.

Mechanically the eye has three degrees of rotational freedom (ϑ, φ, ψ).

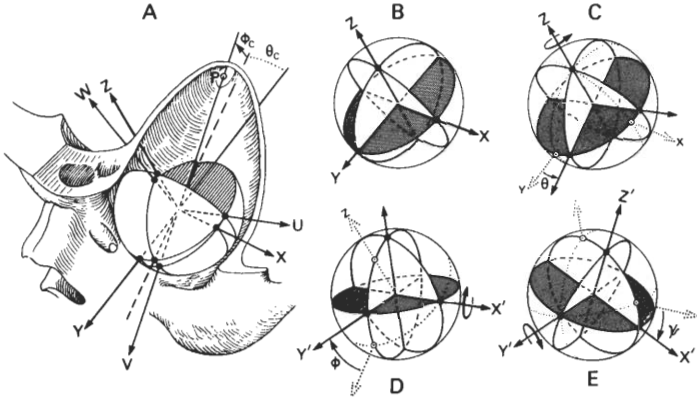

FIG. 1. Coordinate systems. All are for left eyes; all origins are at the center of rotation. (A) Head-fixed coordinates x–y–z and u–v–w. The x–z plane is frontal and y points straight ahead of the subject. The u–v–w coordinates describe the orbital cone. It is similar to the x–y–z system, but rotated through the angles shown so that v is (roughly) the axis of symmetry of the cone. (B–E) Show the sequential development of the eye-fixed coordinates x'–y'–z'. In primary position the x–y–z and x'–y'–z' coordinates coincide. With the unprimed coordinates fixed in the head, and the primed coordinates fixed in the eye, any eye position can be described as a rotation of the primed system about z' through an angle ϑ, followed by a rotation about x' through φ, followed by a rotation about y' through ψ, where the angles are positive as shown in the figure.

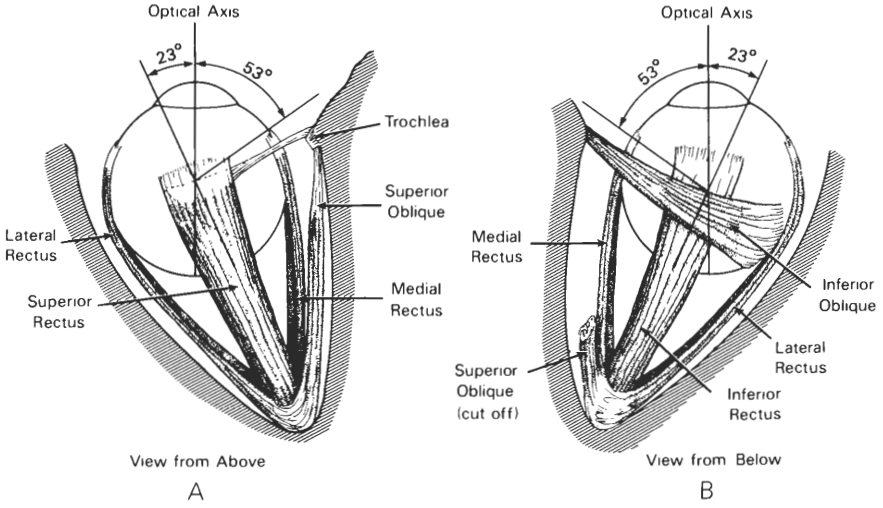

FIG. 2. General arrangement of the left eye and its muscles. (A) View from above. (B) View from below.

However, it is found that for any ϑ and φ the value of ψ is normally always the same, regardless of the path taken by the eye to reach (ϑ, φ). This constraint, reducing the physiologic degrees of freedom to two, is enforced by the brain, which chooses ψ according to Listing's law:

$$\psi = \sin^{-1} \frac{\sin \vartheta \cdot \sin \varphi}{1 + \cos \vartheta \cdot \cos \varphi}. \qquad [1]$$

Listing's law holds for awake, normal eyes; it is violated in sleep (*2*), when the eyes counterroll due to head tilt, and by abnormal eyes.

The eye rests in the orbit surrounded by resilient pads of fat and other elastic structures. The center of rotation of the eye, in consequence, is not fixed but translates slightly as muscle forces vary. In certain pathologic conditions translation may be considerable. The third coordinate system is for describing translation. The *uvw* system is, for the left eye, a left-handed Cartesian system, oriented so that the *v* axis is (roughly) the axis of symmetry of the orbital cone and the *u* axis is horizontal (Fig. 1A).

The tough opaque tissue covering most of the eyeball is called the *sclera*. Each of the six *extraocular muscles* attaches at one end to the sclera (its *insertion*) and at the other end to the bony orbit (its *origin*). Figure 2 shows the origins and insertions of the six muscles with the eye in primary position. Two of the muscles are called *oblique muscles:* the *superior oblique* (SO) and the *inferior oblique* (IO). The remaining *rectus muscles* are the *vertical recti:* the *superior rectus* (SR) and *inferior rectus* (IR), and the *horizontal recti:* the *lateral rectus* (LR) and *medial rectus* (MR). As the brain sees it, that is, in terms of innervations, the six muscles are three *antagonistic* or *reciprocally*

innervated (*2, 3*) pairs: the horizontal recti, the vertical recti, and the obliques. Given the innervation to one member of a pair (e.g., the LR), the innervation to the other (MR) is determined. This simplification is very helpful in modeling: Innervations are usually unknown quantities, which must be solved for, and reciprocal innervation reduces the number of unknown innervations from 6 to 3.

There is no simple way to describe the action of these muscles on the globe! One reason is that, in most eye positions, each muscle inserts in the globe beyond its point of tangency. Normally, there are no firm connections between the muscles and the globe except at the insertion, so that the muscles can slip

TABLE I

NORMAL EYE PARAMETERS

Parameter		LR	MR	SR	IR	SO	IO
Orbital geometry							
Origins (mm)	o_x	−13.00	−17.00	−16.00	−16.00	−15.27	−11.10
	o_y	−34.00	−30.00	−31.76	−31.76	8.24	11.34
	o_z	0.60	0.60	3.60	−2.40	12.25	−15.46
Direct length (mm)	L_x					40.00	
Insertions (mm)	r_{0_x}	10.08	−9.65	0.00	0.00	2.90	8.70
	r_{0_y}	6.50	8.84	7.63	8.02	−4.41	−7.18
	r_{0z}	0.00	0.00	10.48	−10.24	11.05	0.00
Mean radius (mm)	Rad	12.43					
Muscle properties							
Muscle length (mm)	L_0	36.20	31.60	33.90	35.00	32.00	29.10
Tendon length (mm)	l_{tend}	8.40	3.80	5.40	4.80	26.50	1.50
Tendon width (mm)	w_{tend}	9.20	10.30	10.60	9.80	11.00	9.00
Max depart angle (deg)	V_{max}	15.00	15.00	15.00	15.00	15.00	15.00
Sideslip comp (deg/g)	cmp_0	4.00	4.00	4.00	4.00	4.00	4.00
Devel force mult	λ_d	1.00	1.07	0.80	0.97	0.41	0.38
Devel force sens	σ_{iv}	1.00	1.00	1.00	1.00	1.00	1.00
	σ_{dl}	1.00	1.00	1.00	1.00	1.00	1.00
Passive force mult	λ_p	1.00	1.07	0.80	0.97	0.41	0.38
Passive force sens	σ_p	1.00	1.00	1.00	1.00	1.00	1.00
Fascial constants							
Linear stiff (g/deg)	k_p	0.25					
Cubic stiff (g/deg^3)	k'_p	8.1e-5					
Offset (deg)	β_0	0.00		0.00		6.20	
Fat stiffness (g/mm)	*fat*	54.00		27.00		54.00	

Note. The parameters describing orbital geometry and muscle properties are specified for each muscle, listed across the top. Parameters describing the orbital fascia do not relate to particular muscles: β_0 are the rotations about the x, y, and z axes, respectively, that the eye would make with all six muscles detatched (the rest point of the fascial spring); *fat* is the stiffness of the orbital fat to eye translation about the u, v, and w axes, respectively. For derivations of the quantities in Table I not discussed here, see Robinson (*1*).

sideways, restrained somewhat by various elastic connective tissues. We will need to consider muscle sideslip in detail, since the path taken from insertion to point of tangency varies with eye position, and affects the muscle's action. Another difficulty is that, while muscle actions are determined by the geometry of the orbit, specifically the positions of origins and effective insertions of muscles, and the center of rotation of the globe, that geometry is changed by globe translations and muscle sideslip which (completing the loop), are determined by muscle actions. Even though we are concerned here with only the statics of the orbit an analytic solution is hopeless; we must be satisfied with numerical solutions by computer.

Still, it is instructive to intuit a few simple cases. (1) With the eye in primary position, the horizontal recti have very simple actions. Their origins and insertions, and the center of rotation are approximately coplanar: The LR abducts ($+\vartheta$) the eye and the MR adducts ($-\vartheta$) it. Other actions are negligible. (2) If the eye abducts 23° ($\vartheta = 23°$) then, with reference to the $x'y'z'$ coordinate system, the SR mainly elevates ($+\varphi$) and the IR mainly depresses ($-\varphi$) the eye. (3) From a position of extreme adduction ($\vartheta = -53°$) the SO depresses ($-\varphi$) and the IO elevates ($+\varphi$) the eye, although both have appreciable other actions. As may be seen in Fig. 2A, the SO is unique in that it passes through a pulley or *trochlea* which alters its effective origin from its anatomic origin at the orbital apex.

A rough description of eye translation is easy: The four recti pull the eye inward ($-v$), and the two obliques pull it outward ($+v$) and nasally ($-u$).

The muscles are only part contractile tissue, becoming tendonous near their insertions. Except for the SO, whose tendon is 26.5-mm long, the tendons are short (1 to 9 mm), and may be considered inextensible for our purposes. The widths of the tendons (which are the lengths of the insertion lines) are about 10 mm.

The other elastic structures which couple the eyeball to the orbit are the optic nerve, exiting from the back of the eye, and a complex arrangement of elastic sheaths or *fascias,* which we do not consider in detail.

The various orbital and muscular dimensions have been measured in cadavers by Volkman (*4*) and Nakagawa (*5*). Table I contains what we believe to be the most reliable average values.

2. Binocular Vision

One very fundamental function of the visual system is to provide information on the locations of objects in space. The left and right eyes, positioned about 6 cm apart, each form an image of the environment from a slightly different point of view, and comparison by the brain of these two "flat" retinal images yields information about depth. So long as the difference in left and right eye image positions—the *binocular disparity*—is not too large, the *stereopsis mechanism* both interprets the disparity as depth and, by means of *sensory fusion,* causes the disparate images to be perceived singly. Thus, the two eyes must be well

aligned for normal stereopsis. This implies that both accurately fix (that is, image on their foveas in sharp focus) a single point in space.

According to *Hering's law of equal innervation* (see, e.g., *6*), the two eyes are not independently controlled by the brain; changes of innervation are programmed in one of two modes: (1) for a *conjugate* eye movement, in which both eyes rotate through the same angle and in the same direction, or (2) for a *disjunctive* eye movement, in which both eyes rotate through equal angles but in opposite directions. We will only consider conjugate movements, that is, movements to targets in a frontal plane. Then, Hering's law says that fixation of a target by one eye determines the position of the other eye.

Because of the limited range of sensory fusion and the high sensitivity of stereopsis, the open-loop control of binocular alignment described by Hering's law is not accurate enough. Fortunately, in normal vision, both eyes may image the same target and invoke the *motor-fusion* mechanism, which is able to adjust innervations slightly from the dictates of Hering's law so as to bring the fixation target precisely onto the foveae of both eyes. Strabismus, then, becomes manifest only when there is a basic misalignment (due to innervational or mechanical factors) too large to be overcome by motor fusion. We, of course, are interested in this underlying misalignment and, so, must be careful to collect data under conditions in which motor fusion is not possible. Fortunately, this is not difficult: all we need do is arrange that stimuli to the two eyes contain no similar targets which one might fuse. For this purpose two targets are provided: a stationary target, visible to only the *fixing eye,* and a movable target, visible to only the *following eye*. A position of the movable target is sought at which it appears to the patient to be superimposed on the stationary target. A test of this type, the Hess–Lancaster test (or Hess test), is the source of our data on ocular alignment and, therefore, will be modeled. Let us, then, describe this test in more detail.

Using polarized light projectors, and polaroid glasses on the patient, we arrange that a large square grid be visible to one eye only (the fixing eye). The other (following) eye sees only a small line, which can be tilted and moved around on the screen by the patient. It is important that the room be dark so that there are no objects illuminated by unpolarizing light and, so, visible to both eyes. The patient is asked to fix a particular point on the grid, say, 20° to the right of straight ahead and 10° up. This is the "intended eye position" in the sense that the following eye would normally point to this same position. The patient moves his fixing eye so that the image of this point falls on its fovea. We want to know where his following eye has moved (recall that it cannot see the grid). This is the "actual eye position." All we need do is ask the patient to move the small line so that it *appears* superimposed on the selected point. He will move it so that the image of the line falls on the fovea of his following eye, since it will then appear to lie in the same direction as the selected point. Then, the actual positions of the grid point and line on the screen (both of which are visible to the examiner, who does not wear polaroids) show directly where each eye is pointed. Deviations in ϑ and φ are read off the grid. If the patient is

instructed to also rotate the small line to, say, make it colinear with the local grid vertical, torsional misalignments ψ can be measured as well.

Such data are conveniently displayed as "Hess charts," of which Figs. 10 and 11 are examples. Horizontal eye position (ϑ) is plotted on the abscissa (abduction positive) and vertical eye position (φ) on the ordinate (elevation positive). Intended eye positions are marked with crosses, and actual eye positions with circles. The tilt from vertical of an arrow through a circle indicates the deviation of the eye's torsion (ψ) from that prescribed by Eq. [1]. In Figs. 10 and 11 these tilts are multiplied by 5 for visibility.

3. Strabismus

Defects in ocular positioning—strabismus—result from errors in innervation to the muscles, and mechanical abnormalities in the eye, muscles, and orbit.

Strabismus can be congenital or develop later in life; some forms are inherited while others are acquired, sometimes the result of trauma; in some cases strabismus is an isolated abnormality, while in others it is part of an extensive syndrome or is secondary to another disease. The main treatment for strabismus, regardless of its etiology, is eye muscle surgery; various alterations of the muscles and their insertions are made to restore proper eye alignment.

In the United States 83,000 eye operations are performed each year for strabismus (*7*). Acceptable results are achieved in, perhaps, half of these operations, and many patients must return for repeated surgical or other procedures. Some surgical failures may be caused by perverse neural repair mechanisms which respond to the surgical manipulation as though it were damage. The approach we will be discussing is not directly helpful in these cases. In some cases, however, surgical failure is due to a less than optimal choice of the type or amount of surgical manipulation. Given the complexity of orbital mechanics, it is not surprising that intuition is a fallible guide. What *is* surprising is that the clinical literature is all but devoid of quantitative guidelines for strabismus surgeons. A successful model would greatly improve this situation. Further, the scanty data that exist refer, at best, to *average* eyes; if there is reason to believe that a given eye is not average, the data must be modified accordingly. Without an appropriate model there is no way to do this. With increasing use of quantitative diagnostic procedures the ability to *customize* surgery for a particular patient will become increasingly important.

In testing our model against a case of strabismus, the data we usually have to work with are a description of (1) the preoperative misalignments, (2) the surgery performed, and (3) the postoperative misalignments. Deviations are measured by the Hess or some equivalent method. Sometimes additional data are available concerning muscular or fascial stiffness, or innervation. Using a model of the Hess test (see "Binocularity," below), we construct a model of the patient's eyes which shows the same pattern of misalignments as does the patient. This constitutes our *diagnosis* of the patient's disorder. We then do the

same *surgery* on the model eyes as was done on the patient. Finally, we simulate the postoperative Hess test and compare it to that of the patient.

We may, of course, perform any surgery we like on the model eye to see its effect. Eventually, we hope to make predictions that will be used in the planning of surgery.

4. An Early Strabismus Model

Robinson (*1*) developed a model eye for strabismus based on a geometric analysis of the eye, muscles, and orbit, a muscle model, and certain methods of solution. The present model incorporates and extends the geometric analysis and the methods of solution; the muscle model is different. For convenience, we summarize some relevant aspects of the early model below; for a detailed presentation, see Robinson (*1*).

The aim of Robinson's 1975 model was to describe the mechanics of the eye so that one could find the rotational equilibrium position $(\vartheta, \varphi, \psi)$ for a given set of muscle innervations $(iv_0, iv_1, \ldots, iv_5)$ as well as the innervations needed to bring the eye to a given rotational position (translation was not treated). These were called the *position problem* and the *innervation problem,* respectively.

Recall that there are really only three unknowns in either case, since one member of each pair of innervations can be expressed in terms of the other (reciprocal innervation). The rotational equilibrium condition for force balance provides three scalar equations, which are solved by a computer iterative method. At equilibrium, each muscle exerts a total force F_{m_i} (dependent on its stretch δl and innervation iv) which acts to rotate the eye about an axis described by the unit vector $\mathbf{m}_i$. The remaining passive orbital tissues which couple the eye and orbit (fascia and optic nerve) are lumped into a passive force **P.** At equilibrium, then

$$\mathbf{M} = \mathbf{P} + \sum_{i=0}^{5} F_{m_i}(\delta l, iv) \cdot \mathbf{m}_i \qquad [2]$$

equals 0. Since all forces act at the surface of the globe, the common moment arm (approximating the globe as a sphere) can be left out.

The problem is then to express the various rotational forces in terms of eye positions, innervations, and parameters describing the orbit and the muscles. The unit moment vector $\mathbf{m}_i$ of a muscle depends on the muscle's origin O, its point of tangency with the globe T (the "effective insertion"), and the eye's center of rotation C (see Fig. 3).

The center of rotation was taken to be the origin of the xyz coordinates, fixed in the head. From anatomical insertion data ($\mathbf{r}_0$, Table I) and the angles ϑ, φ, and ψ, the rotated insertion was found (R, Fig. 3). The problem was then to find the muscle's path from insertion to the point of tangency T. It was assumed that in primary position each muscle takes the shortest (great-circle) path, while in other positions it does not sideslip enough to do so. No data existed, however, describing these muscle paths and, so, a plausible, mathematically simple path

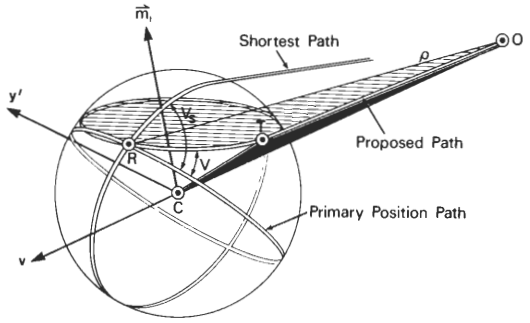

FIG. 3. Possible muscle paths. R is the muscle insertion; C is the center of rotation; T is the point of tangency of the muscle with the globe (it lies on the circle of tangency where all lines from O are tangent to the globe); O is the muscle origin; $\boldsymbol{\rho}$ points from R to O. In primary position the muscle lies along the *primary-position path,* a great circle, and would do so in all eye positions, if there were no sideslip. The *shortest path hypothesis* supposes that the muscles always take a great circle path. The departure angle of this great circle from the primary-position path is V_s. It is proposed that the muscle actually takes an intermediate path, following a small circle that makes an angle V with the primary-position path. The unit moment vector $\mathbf{m}_i$, which is perpendicular to the plane determined by C, T, and O, is the eye's axis of rotation under the influence of the muscle.

was assumed: a (great or small) circle in a plane containing the insertion and origin. The circle was chosen to make an angle V with the path taken in the primary position (Fig. 3). The angle V, the *permitted departure angle,* was found from V_s, the departure angle under the shortest path hypotheses by

$$V = V_s \cdot \cos E, \qquad [3]$$

where E is the angle between the line from C to O and a perpendicular through C to the plane of the primary position path. (This deals nicely with such cases as the LR in 36° adduction, where V_s becomes indeterminate—because all great circle paths are equally short—since $E = 90°$ and so $V = 0$). The unit moment vector $\mathbf{m}_i$ is then perpendicular to the *muscle plane* (the plane containing C, T, and O) with the sense of a right-handed screw, and describes the axis of rotation for that muscle.

If we consider the tendon to be inextensible, then a muscle's longitudinal tension F_m depends on the properties of the fleshy muscle tissue itself. The total force F_m can be considered as the sum of a *passive force* F_p due to noncontractile elastic tissue, and a *developed force* F_d produced by neurally driven contractile elements. F_p is a function of *stretch* δl, the percentage increase in length relative to some standard length. F_d is a function of innervative *iv*, as we would expect, but also depends on δl.

If we suppose that in the normal eye all muscles are qualitatively similar, then both F_p and F_d are proportional to the cross-sectional area of the muscle. This allows us to use the detailed description of the forces of only one muscle (the LR), to derive the forces of the other muscles with *strength* scale factors which represent the ratio of a muscle's cross section to that of the LR.

Length–tension–innervation data were collected by Robinson *et al.* (*8*) and Collins *et al.* (*9*) from patients who were undergoing strabismus surgery. Briefly, their procedure was as follows: A lateral or medial rectus muscle was detached from its insertion and sutured to a strain gauge. It was then stretched to various lengths while the awake patient fixed a series of targets with his other, normal eye. Each fixation, of course, required an appropriate innervation to the fixing eye which, by Hering's law, was supplied as well as to the operated eye. For instance, imagine that the left LR was on the strain gauge. The patient then looked 30° to the left with his right eye. Normally this would have been accompanied by a 30° leftward movement of the left eye which, of course, did not occur. Still, the innervation to the left eye, in particular to the left LR muscle, was the innervation that would have driven a normal left eye 30° to the left, and may be referred to as a +30° (30° abducting) innervation. (There is no practical way to measure the nerve impulses directly.) The left LR was then stretched to several known lengths and the tensions were recorded. The result was a length–tension curve for +30° innervation. This procedure was repeated for several innervations.

Robinson (*1*) computed a weighted average of the length–tension–innervation data then available and found that for each innervation the data could be fit with the same hyperbola, translated an appropriate amount horizontally. This family of length–tension curves is shown in Fig. 4 with stretch, δl, defined as

$$\delta l = 100 \frac{L - L_p}{L_p}, \qquad [4]$$

where L_p is the muscle's length when the eye is in primary position and L is some particular length. Percentage stretch is more convenient than absolute

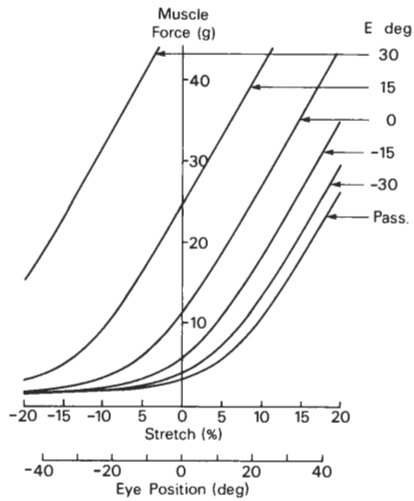

FIG. 4. Length–tension–innervation relationship for a lateral rectus muscle [from (*1*)].

stretch since the same relationship will then hold for muscles of different lengths.

The curve labeled "Pass." (for *passive*) is of special interest. Innervation is assumed to be 0 (returning to our example, the passive curve for the left LR was obtained with the right eye fixing a position to the extreme right), so that this curve describes the passive force F_p. The developed force F_d is then found by subtraction:

$$F_d = F_m - F_p. \qquad [5]$$

δl was found for any given position from the orbital geometry and the calculated muscle path. *iv* was an arbitrary measure, presumably monotonic with effective motoneuron firing rate and, at the outset, unknown. The first solution, then, must be for the innervations, given ϑ, φ, and ψ. One could then supply those innervations to an eye altered, perhaps, to simulate an abnormality or surgical manipulation, and solve for the position of the new eye.

The passive orbital tissues were modeled simply as a homogeneous spring that exerts a recentering force dependent on the eccentricity β of the eye. From measurements taken during strabismus surgery (*8*) this spring was modeled as linear around the origin, hardening at extreme eccentricities.

As a simple example of the use of the 1975 model consider the case in which a normally innervated eye has some mechanical defect and, so, moves to an abnormal position. We want to know where this abnormal eye will point, compared to where a normal eye would point under the same innervations. Let the position of the normal eye be $(\vartheta, \varphi, \psi)$. The first step is to solve the innervation problem. Using the parameters of a normal eye and the position $(\vartheta, \varphi, \psi)$ we can find δl and $\mathbf{m}$ for each muscle and $\mathbf{P}$, the moment of the passive orbital tissues. We then guess values of iv_0, iv_2, and iv_4, and compute iv_1, iv_3, and iv_5 by reciprocal innervation. We then evaluate the total moment on the eye by Eq. [2]. If $\mathbf{M}$ is not 0 we must refine our guess and try again. This iterative procedure continues until $\mathbf{M}$ is acceptably close to 0. We then have found the innervations which would drive a normal eye to $(\vartheta, \varphi, \psi)$.

To what position will these innervations drive our abnormal eye? To find out, we solve the position problem. The procedure is basically the same, except now we guess ϑ, φ, and ψ (an abnormal eye need not obey Listing's law so we cannot calculate ψ from ϑ and φ). We calculate $\mathbf{M}$ by Eq. [2] and, if it is not acceptably near 0, refine our guess and repeat the procedure.

Robinson (*1*) solved many of the problems involved in modeling this complex system, but many problems remained: (1) The muscle force model was unrealistic in having neither a *slack* region when the muscle was sufficiently relaxed nor a *leash* region at extreme stretch, where the muscle resists further stretch. The components of total muscle force F_m, namely, developed force F_d and passive force F_p, very different in their effects on the eye, could not be easily separated in the model. (2) Muscle sideslip was not properly analyzed. (3) As a muscle bends sideways the distribution of force across its width becomes nonuniform and the point at which the distributed force may be thought of as

applied (the centroid) moves toward the stretched edge. (4) Translation of the eye was not treated. It is important both as an output variable (in certain disorders translation along the v axis (Fig. 1A) is an important diagnostic sign) and because of its influence on orbital geometry and, so, on rotations. (5) The model was not binocular: the fixing eye had to be normal (otherwise ψ could not be found and innervations could not be solved for). Often, however, a patient will have both eyes affected or will have surgery on both eyes. (6) The implementation of the model (a Fortran program) was difficult to use and not oriented for use as a component of more complex simulations (such as we will discuss below).

In the model to be described these defects are remedied. A new implementation, called SQUINT, mostly written in C (*10*) and run under the UNIX operating system incorporates many additional features to facilitate use. We will indicate some of these below. A more complete description of the SQUINT system is available from Miller.

First we will describe the changes and additions in the new model, then its various tests and applications, and finally its implementation.

5. Muscle Force

There are two main difficulties with Robinson's hyperbolic curve model of muscle force: It is realistic only for intermediate values of stretch (the so-called *operational zone*), and it cannot be readily modified to simulate abnormal muscles.

If extraocular muscle is allowed to shorten sufficiently it will go slack and exert no force. The hyperbolic model, in contrast, always produces a nonnegligible force. At the other extreme, if a muscle is stretched sufficiently, a point is reached at which stiffness increases dramatically. This so-called *leash* region is not reflected in the hyperbolic model. In the normal eye and under normal conditions the muscles do not enter either of these troublesome regions; they never go slack and the leash region is far enough out (corresponding to about a 50° rotation for the horizontal recti) so that it is not encountered in the normal range of gaze. With abnormal eyes, however, we cannot be so sanguine. The muscle disorder clinicians call a *contracture,* for instance, is characterized by a leash in the normal range of gaze. We will also be interested in modeling an experimental procedure in which the eye is rotated by application of an external force; the region in which one muscle of an antagonistic pair goes slack will be of special interest.

The second difficulty with the old model is that it was often difficult or impossible to alter the normal muscle appropriately to simulate a given disorder. F_p could be changed in a limited way by changing the three parameters of the normal passive hyperbola. F_d, given as the difference of two hyperbolas with the same parameters, could usually not be altered as desired.

The new muscle force model computes total muscle force as the sum of independent developed and passive forces:

$$F_m = F_p + F_d. \quad [6]$$

F_p and F_d, in turn, are derived from passive and developed force surfaces f_p and f_d, respectively:

$$F_p = \lambda_p \cdot f_p(\sigma_p \cdot \delta l) \quad [7]$$
$$F_d = \lambda_d \cdot f_d(\sigma_{\delta l} \cdot \delta l, \sigma_{iv} \cdot iv),$$

where λ_p and λ_d are "scaling" factors and σ_p, $\sigma_{\delta l}$, and σ_{iv} are "sensitivity" factors. These are used to allow the forces of several muscles to be described with a single pair of force surfaces, and to aid in simulating abnormal muscles.

The passive force of a muscle of unit cross-sectional area is a function of percent stretch δl, where

$$\delta l = 100 \frac{L - L_0}{L_0}. \quad [8]$$

L_0 is the length of the relaxed, denervated muscle (mm), and L is some particular length (mm). By definition, F_p is not a function of innervation. The advantage of using L_0 as a reference value rather than L_p (Eq. [4]) is that the multiplicative sensitivity factor σ_p is most useful if $f_p(\delta l)$ goes through the origin. To see this, suppose we want to simulate an abnormally "soft" muscle by setting $\sigma_p < 1$. By the old formulation of Eq. [4], as we stretch the muscle beyond its primary position length, the force at each value of δl is below normal ($\sigma_p = 1$), as we intend. However, if we allow the muscle to shorten below its primary position length, the forces are *higher* than normal. It is hard to imagine a pathology that would alter muscle stiffness in this way. Further, our soft muscle would have a relaxed length ($F_p = 0$) *shorter* than normal; usually, soft muscles *lengthen*. The basic problem with the old formulation is that it defines F_p, an intrinsic property of the muscle, in terms of L_p, which is a property of the orbital mechanism into which the muscle is inserted.

Although there are no existing data that give L_0 directly, we can estimate it using our model, and experimental data on muscle force at primary position length (*8, 9*). These data show that the LR exerts about 1 g of passive force in primary position. Therefore, we adjusted L_0 to produce a primary-position F_p of 1 g for the LR, and F_p values appropriately scaled by λ_p (Eq. [7]) for the other five muscles. These values are given in Table I.

The passive force surface is shown in Fig. 5A. f_p for intermediate stretch ($\delta l = 17$ to $= 40\%$) is derived from a passive force curve similar to that in Fig. 4, based on the data of Robinson *et al.* (*8*) and Collins *et al.* (*9, 11*). This last study reports data obtained from intact normal eyes. It must be admitted that these three data sets are somewhat inconsistent. This is due in part to the extraordinary difficulty in obtaining such data in a well-controlled way, and in part to differences among individual subjects. We have been forced, therefore, to assign weights to the three data sets according to informal judgments of their reliabilities. The curve for intermediate stretch is continued smoothly to the left

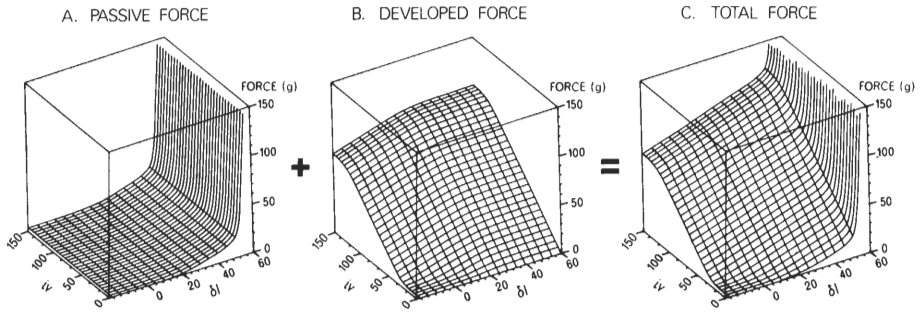

FIG. 5. Forces of a lateral rectus muscle showing leash and slack regions. (A) Passive force F_p. (B) Developed force F_d. (C) Total force F_m. δl is the change in muscle length from L_0 in %; iv is innervation. The intermediate values in these graphs can be generated from Robinson's (*1*) Eq. [39], with $a = 2.77$, $e_0 = -7.9$, and $k = 0.8$. F_p is continued smoothly by hand from $\delta l = 16$, reaching 0 at $\delta l = 0$, to produce the slack region; it is extrapolated by hand from $\delta l = 41$, reaching an arbitrary large slope at $\delta l = 54$, to produce the leash region. Above $iv = 100$, F_d is rolled-off to about 100g for maximum δl, to reflect saturation of the motor units.

by hand, becoming 0 to $\delta l = 0$. To the right, the slope (stiffness) is smoothly increased, reaching an arbitrarily large value for $\delta l = 50\%$.

The passive force surface can be implemented as a table of values of f_p. Abnormal muscles (or normal muscles based on new data) may be simulated by arbitrarily altering this table. In many cases, however, simply manipulating λ_p, σ_p, and L_0 suffices. A *contractured* muscle, for instance, may have a reduced operational zone; it may be fairly normal when stretched, up to, say, 25%, but then encounters the leash. Increasing σ_p by a factor of 2 brings the leash in to about 25% stretch, and decreasing λ_p by a factor of 5 restores a roughly normal stiffness in the (reduced) operational zone. Some contractures may be better simulated by only increasing σ_p.

The developed force of a muscle of unit cross section is a function of innervation iv and, consistent with the sliding-filament model of muscle action, a function of δl, as well.[2] As with the passive force model, we have combined the data of Robinson *et al.* (*8*) and Collins *et al.* (*9, 11*), to arrive at what we believe to be the best estimate of f_d. The developed force surface is shown in Fig. 5B. By definition, $f_d = 0$ for $iv = 0$; the units of iv are arbitrary.[3] It may be useful to try to relate iv to the motoneuron firing rate, but we have not done so. Currently, iv is a dependent variable in the model, and all simulations must at

[2] Developed force should falloff at both small and large δl; only the former is typically seen in human extraocular muscle [(*1, 9, 12,*) see, however (*8*)]. Perhaps the falloff in f_d at large δl is obscured by the sudden rise in f_p. In any case, f_p certainly dominates the total muscle force for large δl.

[3] We choose iv to be consistent with the corresponding variable in Robinson (*1*) (the variable there was $e - e_0$) which has the effect that a given change in iv alters the total force by the same amount as a numerically equal change in δl.

some point solve for the set of innervations, given the description of an eye and its position.

As with f_p, scaling and sensitivity factors are applied to the developed force surface f_d (Eq. [7]): λ_d scales the force, σ_{iv} is the innervation sensitivity, and $\sigma_{\delta l}$ is the stretch sensitivity.

Although each muscle may have unique f_p and f_d surfaces, there are currently no data to require this. For simplicity we assume that forces for the medial rectus, superior rectus, inferior rectus, and inferior oblique can be calculated by scaling the forces in Fig. 5 by the ratio of that muscle's cross-sectional area to the cross-sectional area of the LR. This results in the values of λ_p and λ_d for the normal eye shown in Table I.

6. Muscle Path

For any position of the eye, the force F_m exerted by a muscle acts to rotate the eye about an axis, **m**. To calculate **m**, we need to find the *point* at which F_m may be considered to be applied to the eye. If the muscles were lines or "strings," this would be relatively straightforward: We would find the path on the globe taken by a muscle as it left its insertion, and F_m would be applied to the point at which it was tangent to the globe. However, the muscles are "bands" about 10-mm wide and are tangent to the globe along *line segments*. We will begin by replacing each band with an equivalent string.

To do this we imagine a muscle consisting of many identical independent parallel fibers, each extending the length of the muscle. If each muscle fiber exerts the same force (which we assume is the case with the eye in primary position), the equivalent "string muscle" is easily seen to lie midway between the muscle's edges. As the muscle bends sideways, however, fibers near the outer edge of the bend are more stretched, and so exert more force than fibers near the inner edge; we must determine the point along the muscle's width at which the total force of the muscle may be considered to act. We will call this point the *centroid*.

Figure 6A shows the situation in which muscle fibers are stretched nonuniformly on account of sideways bending through an angle B. Also shown are the total muscle force F_m; the change in length of a fiber due to bending ΔL; and the muscle width w. A z axis (unrelated to that of Fig. 1) lies along the unbent insertion with the origin at the midpoint.

The stress of the unbent muscle is

$$s_0 = \frac{F_m}{w}.$$

We suppose the muscle bends so that the central fiber (at $z = 0$) is unaffected by the bending and, so, is under stress s_0. To find the stress in general we find k, a linear approximation to the muscle's stiffness in grams per millimeter. From Fig. 5C, which is in terms of stretch (grams per percentage L_0) and the resting length of the muscle L_0, we find k as the slope $\partial F/\partial L$ at the current operating

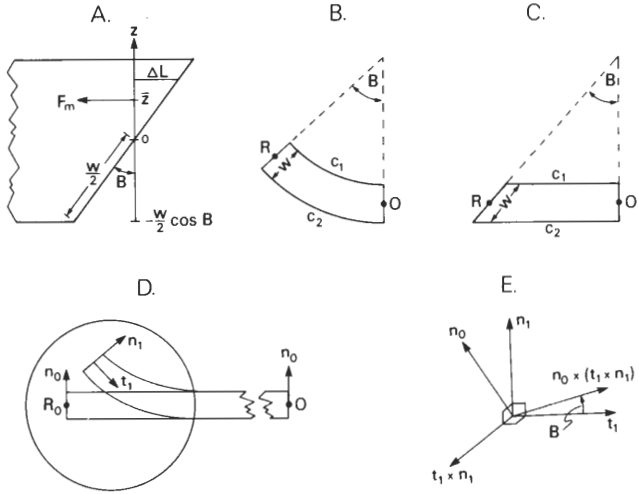

FIG. 6. Calculation of shift of effective insertion (centroid) and angle B of sideways muscle bending (see text).

point. Then, a fiber stretched ΔL more than the center fiber will be under stress

$$s = s_0 + \frac{k}{w}\Delta L = s_0 + \frac{k \cdot \tan B}{w} z.$$

The centroid $\bar{z}$ is found by equating moments:

$$\bar{z} \cdot F_m = \int_{-\frac{w}{2}\cos B}^{\frac{w}{2}\cos B} s(z) \cdot z \cdot dz = \int_{-\frac{w}{2}\cos B}^{\frac{w}{2}\cos B} \left(s_0 \cdot z + \frac{k \cdot \tan B}{w} z^2\right) \cdot dz$$

$$\bar{z} = \frac{k \cdot w^2 \cdot \sin B \cdot \cos^2 B}{12 F_m}. \qquad [9]$$

Thus, the band muscle may be replaced by a string muscle positioned a distance $\bar{z}$ from the center of the band muscle.

Equation [9] shows that the centroid shift $\bar{z}$ is a function of muscle force. Shifting the effective insertions, however, must be expected to alter muscle forces. Consequently, calculation of $\bar{z}$ is an iterative process in which each estimate of $\bar{z}$ alters the muscle path, requiring recalculation of F_m, which leads to another estimate of $\bar{z}$.

Equation [9] supposes that the muscle is straight and lies in a plane, as shown in Fig. 6A. Usually the muscle takes a path that is curved in three dimensions. The important element in Eq. [9] is the difference in the lengths of the two edges of the muscle ΔC, and it can be retained by using an equivalent angle B that estimates ΔC. In general, ΔC depends on the muscle path from insertion to origin, however, a reasonable estimate can be made without considering the

path in detail. Figure 6B shows a muscle of width w lying in a plane, bent along a circular arc of angle B from its origin O to its insertion R. It is easily found that ΔC is independent of the radius of the arc:

$$\Delta C = C_2 - C_1 = w \cdot B. \quad [10]$$

We could, for accuracy, consider the muscle to be a series of arcs, each of angle B_i, but it will be seen that the final effect on calculated eye positions of the centroid shift is small, so that this refinement is unwarranted. To take an extreme case, even if the path of the muscle were straight only a small error would be introduced by Eq. [10]. From Fig. 6C it can be seen that in this case

$$\Delta C = w \cdot\cdot \sin B.$$

For $B = 40°$, Eq. [10] would be only 8% in error. In an arbitrary position of gaze the orientation of the insertion line is given by the "insertion vector" $\mathbf{n}_1$. The "tendon vector" $\mathbf{t}_1$ is tangent to the globe and perpendicular to $\mathbf{n}_1$, as shown in Fig. 6D. $\mathbf{n}_0$, which describes the insertion in primary position, is also shown drawn through O to make the relationship of Figs. 6B and C with Fig. 6D apparent. [The derivations of these vectors are given in (*1*).] The angle of sideways bending B is, then, the angle between $\mathbf{n}_1$ and the projection of $\mathbf{n}_0$ in the plane of $\mathbf{n}_1$ and $\mathbf{t}_1$ or, what amounts to the same thing, the angle between $\mathbf{t}_1$ and the vector $\mathbf{n}_0 \times (\mathbf{t}_1 \times \mathbf{n}_1)$, which is perpendicular to $\mathbf{n}_0$ and in the plane of $\mathbf{n}_1$ and $\mathbf{t}_1$ (Fig. 6E). Thus,

$$B = \cos^{-1}\left(\mathbf{t}_1 \cdot \frac{\mathbf{n}_0 \times (\mathbf{t}_1 \times \mathbf{n}_1)}{|\mathbf{n}_0 \times (\mathbf{t}_1 \times \mathbf{n}_1)|}\right). \quad [11]$$

If, due to surgery, the insertion has a sideways bend B_0 in primary position, we use

$$B = B_0 + \cos^{-1}\left(\mathbf{t}_1 \cdot \frac{\mathbf{n}_0 \times (\mathbf{t}_1 \times \mathbf{n}_1)}{|\mathbf{n}_0 \times (\mathbf{t}_1 \times \mathbf{n}_1)|}\right). \quad [12]$$

Robinson computed a related angle [E in (*1*)] but did not separate sideways bending (about an axis perpendicular to the plane of $\mathbf{n}_1$ and $\mathbf{t}_1$) from "twisting" and "folding" (about axes *in* the plane of $\mathbf{n}_1$ and $\mathbf{t}_1$).

To see if calculating the centroid shift is worthwhile, we found the innervation sets necessary to drive a normal eye to each of 81 points evenly spaced over an 80 × 80° field of gaze. For each gaze position the program started by assuming the centroid to lie at the midpoint of the actual insertion line, calculated the innervations and muscle forces and, using Eq. [9], found a new centroid. It then recalculated innervations, muscle forces, and the centroid, continuing this process to convergence. For each of these innervation sets we then found the position a normal eye would be driven to using (1) a method in which centroid shift was calculated and (2) a method in which centroid shift was ignored and the effective insertion fixed at the midpoint of the actual insertion line.

The first method simply reproduces the original 81 eye positions (a convenient internal check of the program's calculations). The second method shows the errors of ignoring centroid shift as deviations of eye positions from the 81 fixation points. It can be seen from Fig. 7A that these errors are small for the normal eye, tending to increase with eccentricity. Whether the centroid calculation is worthwhile will depend on the application. It will tend to be more important in cocontractive and restrictive syndromes, in which large muscle forces (F_m, Eq. [9]) exist.

We now return to consider the path taken by a string muscle (here we include the tendon) as it runs along the surface of the globe, from its point of insertion to its point of tangency. Recall (Fig. 2) that in primary position all of the muscles insert into the globe *beyond* the globe's center of rotation. As the globe rotates to arbitrary positions, then, we expect the muscles to slip sideways. The horizontal recti, for instance, should slip upward as the eye elevates and downward as the eye depresses. If sideslip were unrestrained, a muscle would simply take the shortest path on the globe (a great circle) from insertion to point of tangency (Fig. 3). Early analyses by Krewson (*13*) and Boeder (*14*) assumed that this was the case. However, elastic connective tissue surrounds the muscles and joins them to each other, forming a sort of cap anterior to the equator of the globe, which reduces sideslip. Robinson (*1*) supposed that muscles sideslipped only a fraction of the way toward the shortest path.

To model muscle sideslip correctly one would approach it as a distributed problem shown in Fig. 8A. Instead of letting the eye rotate up while holding the origin fixed it is easier to visualize things if the eye is still and the origin moves up from O to O'. The muscle is pulled sideways off its primary position path. A distributed fascial spring represented by little incremental springs acts to prevent sideslip. Any element of tendon, ds, has three forces acting on it: the tendon tension pulling it toward the insertion R, that pulling it toward O', and

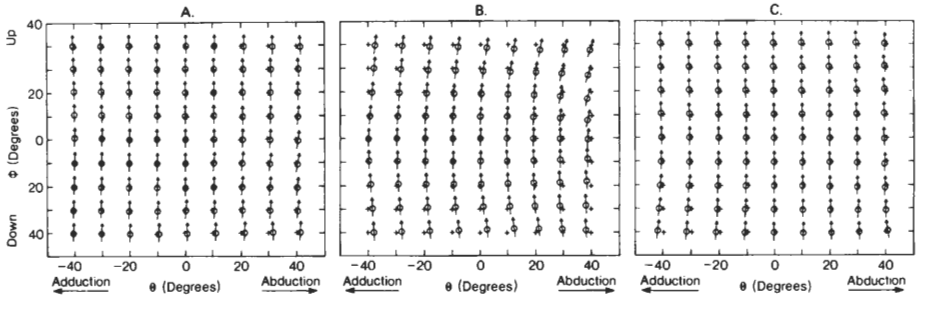

FIG. 7. Sensitivity of eye positions to alterations in the calculations. In all cases, innervations are supplied that would drive a normal eye (showing centroid shift, sideslip, and translation) to the positions indicated by the crosses. The circles show the positions of simulated eyes altered in specified ways; the deviation of each circle from its corresponding cross shows the eye position error in ϑ and φ. The tilt of the associated arrow from straight up shows the deviation from normal torsion (tilts multiplied by five for visibility). (A) Effective insertion is fixed at the center of the insertion line. (B) The departure angle V is fixed at 0. (C) The eye is not allowed to translate.

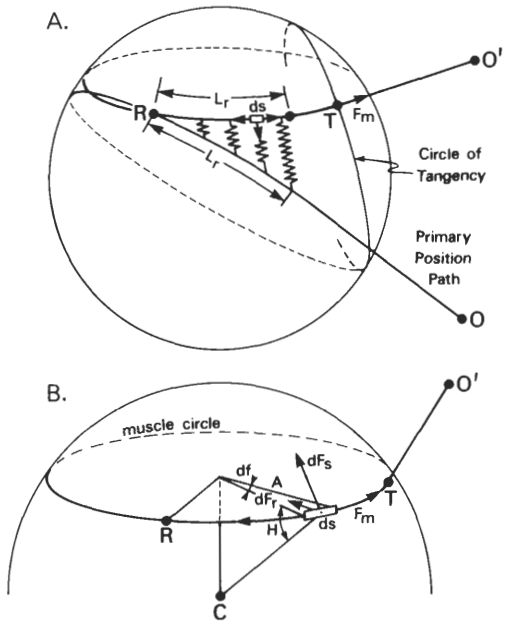

FIG. 8. Calculation of muscle sideslip (see text).

the spring element pulling it back toward the primary-position path. Force balance imposes a constraint on the local curvature which leads to a differential equation. Its solution, with suitable boundary conditions, describes the tendon's path. The problem of the suspension bridge is a classical, if simple, example. Given that the springs are nonlinear and the path is curved in three dimensions, not two, this is obviously a formidable problem not likely to be solvable in closed form. A computer simulation by quantizing the tendon into n points and solving n nonlinear simultaneous equations also seems a burdensome addition to the calculation not commensurate with improved accuracy, especially given our lack of knowledge about the springs.

Consequently we continued the approximation of Robinson (*1*) that the path is part of the circle (the muscle circle) formed by the intersection of the globe's surface with a plane that contains the insertion R and the origin O. Any such plane crosses the circle of tangency at right angles and one is selected that makes the angle V with the primary position path (Fig. 3). Given this approximation how does one find V? In Robinson's calculations V was independent of total muscle force F_m. This cannot be correct; clearly an increase in F_m will act to increase V. In order to introduce this influence, we find the contribution of F_m to the sideslipping force.

In Fig. 8B, the component of F_m directed toward the center of the muscle circle on each end of the path element ds is $F_m \cdot \sin(df/2)$ or approximately $(1/2)F_m \cdot df$. Together, the radial force F_r is

$$dF_r = F_m \cdot df = \frac{F_m}{A}\, ds,$$

where A is the radius of the muscle circle. The component of dF_r tangent to the globe and perpendicular to the tendon path is

$$dF_s = \sin H \cdot dF_r = \frac{F_m \cdot \sin H}{A}\, ds, \qquad [13]$$

where H is the angle between the plane of the muscle circle and any radius drawn from C to the muscle circle (see (1) for the derivations of A and H).

The force dF_s acts to pull the muscle sideways and is equivalent to the distributed loading force in Fig. 8A that is opposed by the incremental springs and determines the shape of the actual path. It is constant and independent of s only because we have forced the path to be circular. The true relation between dF_s and path shape is unknown and our choice of a circle effectively causes the path to be represented by a single variable V. The springs in Fig. 8A will also be lumped into a single spring relating V to a lumped measure of sideslipping force. If L_g is the length of the arc of contact with the globe, then

$$F_s = \int_0^{L_g} \frac{F_m \cdot \sin H}{A}\, ds = \frac{F_m \cdot L_g \cdot \sin H}{A}. \qquad [14]$$

Now F_s is related to V through a nonlinear spring:

$$V = V_{\max} \cdot \left(1 - e^{-\frac{cmp_0}{V_{\max}} F_s}\right), \qquad [15]$$

where $V_{\max}$ is the asymptotic, or maximum, departure angle allowed and cmp_0 (degrees/gram) is the compliance of the spring for small F_s. $V_{\max}$ and cmp_0 will be varied until V approximates experimental data.

Experimental observations on muscle sideslipping (Miller and Scott, unpublished observations) provide a basis for setting the constants in Eq. [15]. Radiopaque markers were implanted in two monkeys along the upper and lower margins of the LR of one eye, taking care to minimize damage to the intermuscular tissues. A scleral search coil was implanted in the other eye using a method that does not tend to induce strabismus (*15*). Conventional (parallel projection) X-ray exposures were made to visualize the LR in lateral view, with the eye in different positions of gaze. Observations reveal that the LR sideslips through a range no larger than $\pm 10°$ over a 50° square field of gaze. The results of this study were well simulated by setting $V_{\max}$ equal to 15° and cmp_0 equal to 4.0.

Note that, as with $\bar{z}$ and F_m, V and F_m are mutually dependent, so that each estimate of F_m in an iterative process requires a reestimate of V.

Following the method used above to evaluate the centroid calculation, we show in Fig. 7B the substantial errors that result from assuming the departure angle V to be fixed at 0 in a normal eye. Note that this still permits some sideslip, since the point where the muscle's path leaves the globe will still move

sideways with respect to its position on the globe in primary position. However, this is the least amount of sideslip compatable with the approximations of our model.

Because the muscles insert beyond the center of rotation and are able to slip sideways, an antagonistic muscle pair may develop "bridle" forces (*1*). Contraction of the horizontal recti, for instance, will tend to raise an eye in upgaze and depress it in downgaze. Bridle forces create nonlinearities that complicate eye movement control, but other mechanical effects might reduce or cancel them. If muscles took the shortest path (Fig. 3), the point of tangency would move several tens of millimeters in some gaze positions (*1*), producing very large bridle forces. Depending on the model adopted, sideslip might vary between such implausibly large values and zero. Clearly, a proper analysis of sideslip is the main requirement for estimating the bridle force. The present analysis (supported by the data of Miller and Scott) predicts small, but nonnegligible, bridle forces. When the eye is elevated 30°, for instance, 15% of the force of the MR acts to elevate the eye.

France and Burbank (*16*) have suggested that centroid shifts, more than canceling, actually reverse large bridle forces produced by muscle sideslip. Our calculations show, in contrast, that shifts of the effective insertion (and, so, of the point of tangency) due to nonuniform stretching are no more than about 1 mm over a 60° square field of gaze, so that this is not an important factor. The important thing is to model muscle sideslip correctly in the first place, since variations in the sideslip model can produce shifts in the point of tangency an order of magnitude larger than those due to centroid shifts.

To summarize: The band muscle is replaced by an equivalent string muscle, accounting for nonuniform strain caused by sideways bending. This equivalent string describes a circular arc path on the globe from its effective point of insertion to its effective point of tangency, and then proceeds straight to the origin. The muscle path is contained in a plane which passes through the insertion and the origin, and makes an angle V with the muscle's primary-position path (see Fig. 3).

Having described the muscle's path, we can find the vector $\mathbf{m}$ about which the eye tends to rotate: it is perpendicular to the plane determined by the eye's center of rotation, the muscle origin, and the point at which the muscle is tangent to the eye.

7. Globe Translation

We have been considering the eye's center of rotation to be fixed. The eye is surrounded by resilient pads of fat, however, and can translate several millimeters, as one can verify by pushing on one's eye through the eyelid. Certain disorders are characterized by large translations of the globe (usually retraction into the orbit) when certain movements are attempted. This may occur, for example, because an antagonist is too stiff to stretch when its agonist contracts,

or because of actual cocontraction of antagonistic muscles, as in Duane's syndrome (*17*).

Because of its diagnostic value, globe translation is of interest as an output variable of our model. Moreover, translation is important insofar as it affects eye rotation. Obviously, globe translation alters the degree of stretch of the muscles and, thus, the muscle forces F_m. Translation also alters the position of the globe relative to the muscle origins and, so, alters the axes of rotation **m**.

Accounting for translation in the model is straightforward. Figure 1A shows the orientation of the *uvw* coordinate system, by which we measure translation. We are mainly interested in calculating translation along the v axis, although we get translations along u and w as well. Point C is the center of rotation of the eye and P is the apex of the muscle cone, which we have taken to be midway between the origins of the SR and IR (at $[-16.00, -31.76, 0.60]$ in the *xyz* system). The *uvw* system is related to the *xyz* system by rotations:

$$\begin{aligned} \vartheta_c &= \cos^{-1}(\mathbf{y} \cdot (\mathbf{u} \times \mathbf{z})) \\ \varphi_c &= \cos^{-1}(\mathbf{v} \cdot (\mathbf{u} \times \mathbf{z})), \end{aligned} \qquad [16]$$

and the coordinate transformation $(x, y, z) \rightarrow (u, v, w)$ is given by

$$A = \begin{pmatrix} \cos \vartheta_c & \sin \vartheta_c \cdot \cos \varphi_c & -\sin \vartheta_c \cdot \sin \varphi_c \\ -\sin \vartheta_c & \cos \vartheta_c \cdot \cos \varphi_c & -\cos \vartheta_c \cdot \sin \varphi_c \\ 0 & \sin \varphi_c & \cos \varphi_c \end{pmatrix}. \qquad [17]$$

In the normal orbit $\vartheta_c = 26.8°$ and $\varphi_c = -1.4°$.

To calculate translation, then, we go through the following steps: (1) Find the x, y, and z components of the six muscle forces and sum them. (2) Using ϑ_c and φ_c calculated in Eqs. [16], transform the summed muscle forces to the *uvw* system operating with A (Eq. [17]). (3) Calculate translation of the globe center along the u, v, and w directions according to a linear model in which the orbital fat has the stiffnesses shown in Table I (*fat*). The most important of these is the stiffness along the v axis of 27 g/mm (*18*). (4) Transform the translation from *uvw* to *xyz* coordinates by operating with A^{-1}. (5) Because we use the globe center C as the origin of our coordinate systems (Fig. 1), it is convenient to imagine that the *origin* moves rather than C. Therefore, subtract the calculated shifts from the origins o_x, o_y, and o_z (Table I). (6) Recalculate muscle forces.

As with the centroid, translation is determined by, and determines, muscle force. We assume the anatomical position of the globe center (with the muscles exerting no forces) and calculate muscle forces. From these forces, we calculate a new globe center, repeating these steps until the process converges.

The significance of the effect of translation on rotation can be assessed as before. Figure 7C shows the errors in rotation that would result from ignoring globe translation in a normal eye. These errors are small for a normal eye. In abnormal eyes, especially those with restrictive or cocontractive syndromes (in

which globe retraction is observed clinically), very large errors might result from ignoring translation.

Our computer program performs the calculations described here and by Robinson (*1*), iteratively varying either iv (for the innervation program) or (ϑ, φ, ψ) (for the position program) until the residual moment **M** (Eq. [2]) is tolerably close to 0. However, F_m (Eq. [6]), one of the last values to be calculated (dependent as it is on both muscle length and innervation), affects values used earlier in the calculation: muscle origins o must reflect globe translation, insertions r are displaced by $\bar{z}$ (Eq. [9]) because of the nonuniform distribution of stress across the tendon, and the departure angles V (Eq. [15]) change with each recalculation of the sideslipping force F_s (Eq. [14]). Thus, minimizing **M** is not a sufficient criterion for convergence; we must also check that various other values (currently, F_m (g), V(deg), iv, and $\delta l(\%)$) are stable across iterations. We require that each of these 24 values be stable within 0.02. Each component of **M**(g) must be less than 0.02.

If the same eye parameters (Table I) are used with both, the innervation and position programs are inverse operators. The overall accuracy of the innervation and position programs together, then, can be gauged by running the innervation program on a field of eye positions, and then the position program on the output of the innervation program. For the 81 positions we used in Fig. 7, no component of position is in error by more than 0.01°.

With the parameters described, the innervation calculation converges in an average of 10 iterations per point, and the position calculation, in an average of 8 iterations per point. We have implemented a "fast" version of the program, which eliminates the translation and centroid calculations, and also relaxes convergence requirements by a factor of 50; this speeds the program by a factor of 2.5. The maximum error in the "inversion" test rises to 0.30° on account of relaxed convergence requirements; the errors incurred by ignoring the centroid and translation calculations will usually be larger.

The innervation program runs faster than the position program. This difference is largely due to the methods of guessing the next innervation set and eye position, respectively, on each iteration. In the innervation program, a good guess at the next innervation to try can be obtained by making a linear expansion of Eq. [2] around the current iv, and then finding Δiv to bring **M** to 0. (see (*1*); Eqs. [46]–[54]). In the position program, however, we see no way to arrive at a quick, accurate guess at the next position. Robinson ((*1*); Eqs. [59]–[60]) simply resolved the residual moment **M** into ϑ, φ, and ψ components and divided each component by a constant that was an estimate of the eye's overall stiffness. This yielded a rough guess at the next eye position. This method converged slowly, especially for pathological eyes in which the overall stiffness constant was badly in error.

Our present method of guessing the next trial eye position involves taking small steps in ϑ, φ, and ψ around the current position, in order to estimate the stiffness of the eye. The stages of this calculation are (1) Make a rough guess at $\Delta\vartheta$, $\Delta\varphi$, and $\Delta\psi$ using the method of Robinson (*1*). After the first iteration, we

can use the diagonal elements of the **K** matrix, derived below, instead of the "overall stiffness constant" (currently, 1.5 g/degree).[4] If $\Delta\vartheta$, $\Delta\varphi$, or $\Delta\psi$ is larger than about 10°, we cannot improve on the old method. This is because, when the eye is far from equilibrium its behavior is very nonlinear, and the matrix method we are developing is inappropriate. By the second iteration, though, we are usually close enough to proceed as follows: (2) Step away from the current eye position by $(\Delta\vartheta', 0, 0)$, and compute the change in the residual moment $(\Delta M'_{\vartheta\vartheta}, \Delta M'_{\varphi\vartheta}, \Delta M'_{\psi\vartheta})$. (3) Repeat for steps $(0, \Delta\varphi', 0)$ and $(0, 0, \Delta\psi')$, to find the stiffness matrix **K**:

$$\begin{pmatrix} \Delta M'_{\vartheta} \\ \Delta M'_{\varphi} \\ \Delta M'_{\psi} \end{pmatrix} = \begin{pmatrix} K_{\vartheta\vartheta} & K_{\vartheta\varphi} & K_{\vartheta\psi} \\ K_{\varphi\vartheta} & K_{\varphi\varphi} & K_{\varphi\psi} \\ K_{\psi\vartheta} & K_{\psi\varphi} & K_{\psi\psi} \end{pmatrix} \begin{pmatrix} \Delta\vartheta' \\ \Delta\varphi' \\ \Delta\psi' \end{pmatrix}.$$

(4) Invert **K** to get the compliance matrix **C**. (5) The change in eye position estimated to bring **M** to 0 is then gotten from:

$$\begin{pmatrix} \Delta\vartheta \\ \Delta\varphi \\ \Delta\psi \end{pmatrix} = \begin{pmatrix} C_{\vartheta\vartheta} & C_{\vartheta\varphi} & C_{\vartheta\psi} \\ C_{\varphi\vartheta} & C_{\varphi\varphi} & C_{\varphi\psi} \\ C_{\psi\vartheta} & C_{\psi\varphi} & C_{\psi\psi} \end{pmatrix} \begin{pmatrix} \Delta M_{\vartheta} \\ \Delta M_{\varphi} \\ \Delta M_{\psi} \end{pmatrix}, \qquad [18]$$

where the ΔM's are the unresolved moments at the current iteration step. (6) Finally, the new estimate of eye position is $(\vartheta + \Delta\vartheta, \varphi + \Delta\varphi, \psi + \Delta\psi)$.

8. Binocularity

The Hess test involves both eyes. To simulate the test we wish to (1) choose positions for the fixing eye. These correspond to where the patient is asked to look on the grid visible only to the fixing eye. Then, for each fixing-eye position, we wish to (2) calculate the innervation set to the fixing eye, (3) the *corresponding* innervation set to the following eye and, finally, (4) the position of the following eye. Two problems complicate this simulation.

The first arises when we try to find the innervations to an abnormal eye fixing a known position (ϑ, φ) on the screen: What is the value of ψ? Listing's law (Eq. [1]) cannot help us directly, since the fixing eye is not normal. ψ, of course, depends on the innervations, but they are what we are trying to find!

This knot is untied by recalling that Listing's law is really a constraint on the pattern of innervations and not on the mechanics of the orbit itself. If it is only the fixing eye that is abnormal, and not the innervations, then the latter are still *Listing innervations,* that is, innervations which would drive a normal eye so that it obeyed Listing's law. We can generate any Listing innervation set by solving the innervation problem for a normal eye and some point $(\vartheta, \varphi, \psi)$,

[4] This is an overestimate of normal eye stiffness, which is close to 1.0 g/degree. However, it causes the iterative procedure to take small, conservative, steps, avoiding the oscillations that sometimes occur when solving for a position near the leash region of a muscle.

where (since this is a normal eye) ψ is given by Eq. [1]. For each Listing innervation set, we can solve the position problem for the abnormal eye, giving ϑ, φ, and ψ. We could proceed, by trial and error, to generate Listing innervation sets until we found one which drove the abnormal fixing eye to the desired point (ϑ, φ) and, thereby, find the corresponding ψ. A less costly method will suffice to find a value of ψ to go with any (ϑ, φ) for the abnormal fixing eye: (1) Generate a field of normal eye positions, that is, sets (ϑ, φ, ψ) where ψ is given by Eq. [1]. Values of ϑ and φ at 10° intervals over a field 80° square (81 points) are reasonable. (2) Solve for the innervation sets which would bring a normal eye to each position in the field. These are Listing innervation sets. (3) Find the position (ϑ, φ, ψ) the abnormal fixing eye would move to under each Listing innervation set. With respect to the abnormal eye and Listing innervations, these points form a *fixable field*. Note that, in general, the projections of the points (ϑ, φ, ψ) on the *ϑ–φ plane* will not form a regular rectangular array. Still, the fixable field defines a surface $\psi(\vartheta, \varphi)$. (4) For each position (ϑ, φ) of the fixing eye we find the corresponding ψ by interpolation. Algorithms for performing this interpolation are available (*19*). The entire procedure is shown schematically in Fig. 9A.

It is worth mentioning that, with appropriate changes, the above procedure could be used for cases in which innervations were abnormal due to, say, a brainstem disorder. The abnormality would presumably be described with reference to the normal, Listing innervations. Duane's syndrome, for instance, is due to congenital absence of the abducens motor nucleus, which normally innervates the LR. The nerve which normally innervates the MR, somehow comes to innervate the LR as well (*17*). This results in cocontraction of the LR and MR when adduction is attempted in the affected eye. To simulate this we need only insert between steps 2 and 3 above, the following: (2.5) For each innervation set, replace the LR innervation with the MR innervation (or some fraction thereof, depending on the strength of the perverse innervation).

To continue with the Hess test simulation, for each (ϑ, φ, ψ) of the fixing eye we solve the innervation problem for the fixing eye (Fig. 9B). We then want to supply "corresponding" innervations, according to Hering's law, to the following eye and calculate its positions.

The second complication is the proper treatment of Hering's law. Since the normal structure of the two eyes has mirror symmetry, a coordinated (conjugate) movement (say, to the upper right) will involve different innervations to the muscles in the two eyes. The direct mapping of fixing-eye innervations into following-eye innervations is unknown. However, we do know the mapping of fixing-eye positions to following-eye positions for normal eyes:

$$\begin{aligned} \vartheta_{fol} &= -\vartheta_{fix} \\ \varphi_{fol} &= \varphi_{fix} \\ \psi_{fol} &= -\psi_{fix}. \end{aligned} \qquad [19]$$

That is to say, if we assume the neural mechanisms that program innervations

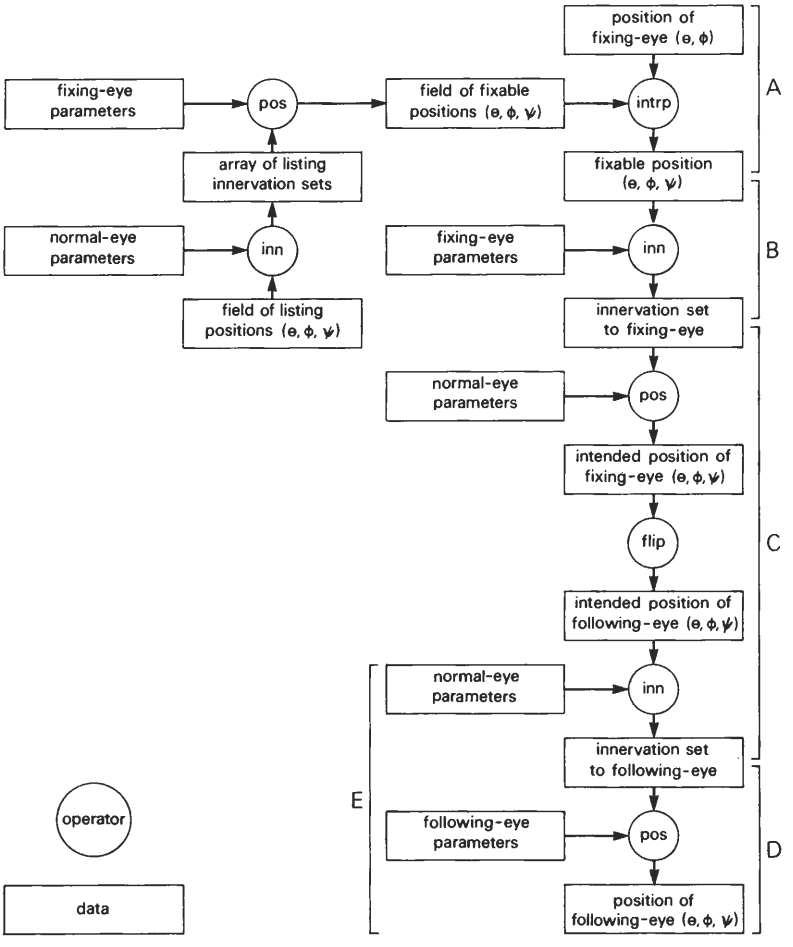

FIG. 9. Operators and data involved in the general binocular case. "inn" is an operator that computes innervation sets ($iv_0, \ldots, iv_5$), given the description of an eye and positions (ϑ, φ, ψ) it is to fix; "pos" computes eye positions, given the parameters of an eye and innervation sets; "intrp" performs interpolation on a surface, finding ψ to go with (ϑ, φ). "flip" reflects eye positions across the midline according to Eq. [19]. (A–D) Phases of the full binocular simulation, as described in the text. (E) Abbreviated solution possible if the fixing eye and the brainstem are normal.

to be normal, that is, unaffected by any abnormalities of the eyes, we can: (1) find the position to which the brain intends the (supposed normal) fixing eye to go, (2) find the mirror-symmetric position by Eqs. [19] to which, under Hering's law, the brain intends the following eye to go, and (3) find the innervations supplied by the brain (under it's assumption that the following-eye is normal). The procedure is diagrammed in Fig. 9C.

Finally, the Hess test simulation is completed by solving for the positions of the following eye (Fig. 9D).

The roles of fixing and following eyes may then be interchanged, as in the clinic.

In light of the cumbersome nature of the full binocular solution, we should point out that if everything is normal except for the following-eye mechanics, most of the above complications are avoided. In this case, for each fixing-eye position, the innervations to the following eye can be found by (1) solving the innervation problem for a normal eye and the position a normal following eye would take, and (2) supplying that innervation set to the (abnormal) following eye, to find its position. This abbreviated procedure is indicated as Fig. 9E.

9. Diagnosis

Many kinds of information are considered by an ophthalmologist in arriving at a diagnosis of strabismus. But, regardless of the clues used to reach it, the diagnosis itself is (or should be) a hypothesis about abnormalities of orbital mechanics or innervations. One way in which our model can serve as a diagnostic aid is to allow the physician to test his diagnosis; to see if the suspected abnormalities are sufficient to produce the pattern of misalignment found in the patient. Parameters of the model are modified to reflect the diagnosis, and a model Hess chart is produced for comparison with that of the patient. If there is a discrepancy, the diagnosis may be altered and the process repeated until a satisfactory match is achieved.

It should be apparent that many aspects of the model can be manipulated in pursuit of a diagnosis. Any of the data boxes in Fig. 9 may be modified, as can the muscle force surfaces in Fig. 5. However, the following cautions apply: (1) A solution may not exist in certain cases. Despite the fact that we always arrive at three equations in three unknowns, because of the nonlinear nature of the system and the restrictions on possible solutions (position coordinates must be real numbers and innervations must be positive numbers), it is not difficult to find situations in which the iterative solution of Eq. [2] does not converge. It is possible to find positions (ϑ, φ, ψ) for instance, which are nonfixable in the sense that an innervation set cannot be found which brings the eye to (ϑ, φ) simultaneously producing a torsion ψ. (2) The modifications should be interpretable in physiologic terms or they will not constitute a diagnosis.

A common clinical situation involves mechanical abnormalities in a single eye. Let us assume that Hess-chart data are collected with the good eye fixing and the abnormal eye following; this allows the much abbreviated simulation procedure described at the end of the previous section to be used. Also, all of the diagnostic modifications will be changes in the values of the parameters of the following eye (see Table I). Note that certain abnormalities of innervation can be modeled as changes in muscle strengths (λ_d and λ_p) and sensitivities (σ_{iv}, $\sigma_{\delta l}$, and σ_p). For these cases it is feasible to have the computer suggest diagnoses, by allowing it to search for the values of following-eye parameters which minimize the differences between the model and patient Hess charts. Such

automatic parameter searching has been implemented using a straightforward, though costly, iterative method.

Clinical experience and professional judgment are in no way supplanted by the parameter searching program. The number of parameters in the search can be limited to those felt most pertinent in each case. It is best to fix as many eye parameters as possible, either on the basis of direct measurement (see below) or presumption (usually of normality). The parameters allowed to vary should be given initial values which represent one's best guesses. One must be prepared to reject physiologically implausible solutions.

10. Surgery

Whether the underlying abnormality is in the brain or in the orbit, the most common treatment for strabismus is surgery on the extraocular muscles. Such surgery consists of mechanical manipulations which can be described as changes in the eye parameters of our model.[5] There are three types of surgery commonly performed.

The first type changes a muscle's insertion. The muscle is cut from the globe at its insertion and sewn back onto the globe at another point. This may affect both the degree of stretch δl of the muscle and its unit moment vector $\mathbf{m}$ for any given eye position. Such surgery is called *recession, advancement,* or *transposition* depending, respectively, on whether the main effect in primary position is to decrease δl, increase δl, or change $\mathbf{m}$. These surgeries are simulated by changing the coordinate of the insertion (r_{0_x}, r_{0_y}, r_{0_z}) in Table I.

The second type of surgery is called *resection:* the muscle is disinserted, a length is cut off (this may be only tendon or may include contractile tissue), and it is then sewn back to its original insertion. The changes to Table I would be in the length of the tendon and, with a large resection, might include a change in relaxed muscle length, L_0.

Finally, tenotomies involve a cut through the tendon. *A complete tenotomy* is really a large recession, since the severed muscle relaxes back into the orbit and eventually *reattaches* itself to the globe at a point nearby! More interesting from our point of view is the *partial tenotomy* in which a cut extends from one edge only part way to the other. Its simulation depends on where it is performed. If done at the insertion, the muscle will relax a bit as the cut edge of the tendon rotates about the intact portion. The tendon then reattaches itself to the globe in this new position. We simulate this as a small recession and a twist of

[5] The manipulations are clearly mechanical; however, it is possible that their effects are more complex. For instance, there exist mechano-receptors (muscle spindles and tendon organs) in each human extraocular muscle which provide the brain with information concerning the length of the muscle or its load. The brain might respond to this information by altering the innervation to one or more of the muscles. Thus, a surgical manipulation of the orbit might stimulate the muscle spindles thereby altering innervations. This effect would interact with the direct mechanical effect of the surgery in determining eye alignment. At present, little is known about the function of extraocular muscle spindles. If they turn out to have a role in strabismus, it should be possible to include their effects in the model.

the line of insertion (B_0, Eq. [12]). A partial tenotomy that is too far from the insertion for the cut end to reattach to the globe (if the contractile tissue is cut, it is called a *myotomy*) should probably be modeled differently, as a relaxation of the muscle and, perhaps a shift of the effective insertion point along the insertion line toward the intact edge. For the most common procedures, our program provides commands that take the minimum information necessary (e.g., muscle name and amount of surgery) and perform the necessary calculations for the new values of the parameters in Table I.

11. A Case of Superior Oblique Palsy

In this section, many of the ideas discussed above will be illustrated, as we show how the model is actually used to analyze a case of SO palsy.

This disorder is a good one for our purposes because, in one way, it is quite complex: because of the complex action of the SO, its paralysis results in horizontal, vertical, and torsional misalignments which vary over the field of gaze. It is interesting to see if the model can simulate all of the features of this disorder.

With respect to its underlying cause, however, a SO palsy can be fairly simple. It can result from relatively mild trauma and, so, have a sudden onset in otherwise normal adults. The paralysis in such cases arises from damage to the fourth cranial nerve which innervates the SO. This nerve takes a circuitous route from the brainstem to the orbit and is often damaged by blows to the head too mild to have other serious effects.

Our simulation plan is to (1) adjust eye parameters in the model to simulate the preoperative misalignments shown by the patient. It will be interesting to see how well we can do this. However, the success of a preoperative simulation cannot be considered a strong test of the model, since we have many free parameters and usually cannot verify the parameter values assigned. (2) Then, we will perform surgery on the model and compare the model outcome to the actual outcome of the patient's surgery. Predicting the outcome of surgery *is* a good test of the model, since we are constrained to do to the model exactly what was done surgically to the patient.

Our patient[6] is an otherwise normal 59-year-old woman who fell from a bicycle, sustaining a SO palsy on the right side. There was no damage to the orbit and it is presumed that intracranial damage to the fourth nerve had occurred. Scott determined, by electromyography, that the right SO was indeed completely denervated.

The Hess chart in Fig. 10A was taken with the patient's normal left eye fixing and her paretic right eye following. Horizontal eye position in degrees is shown on the abscissa, with abduction to the right; vertical eye position is shown on the ordinate. The "+" signs are the positions of attempted fixation, that is, where her right eye would have gone if it had been normal. The corresponding

[6] These data were kindly provided by Dr. Alan B. Scott of the Smith–Kettlewell Institute of Visual Sciences in San Francisco.

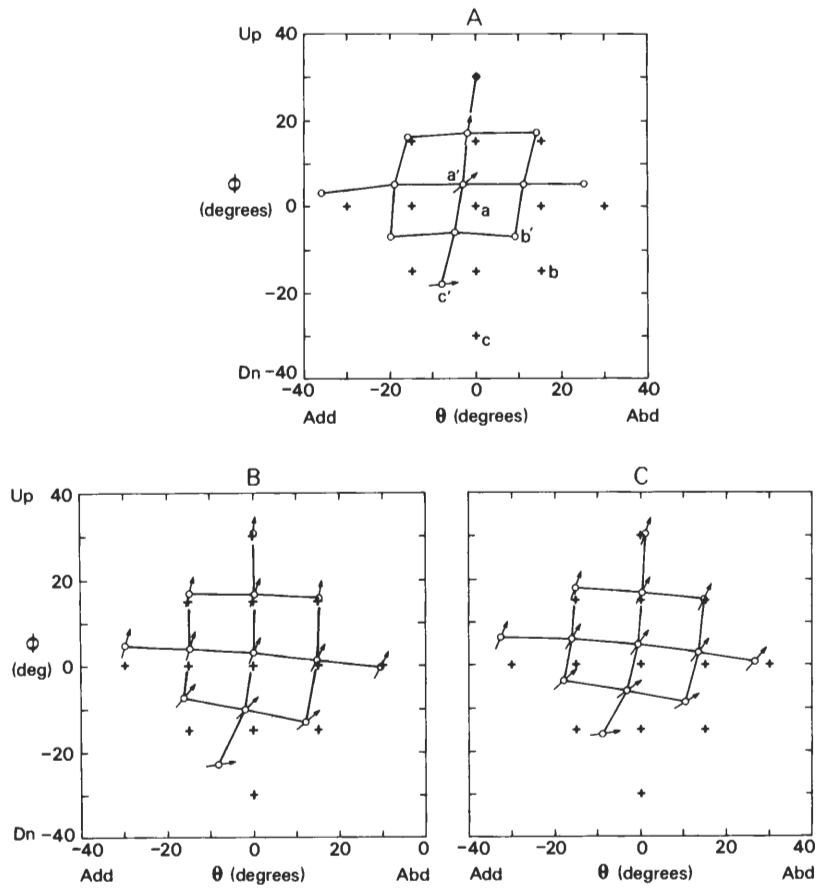

FIG. 10. Preoperative Hess charts, showing positions of paretic right eye moving passively with normal, fixing left eye. Abscissa is horizontal eye position ϑ (abduction positive); ordinate is vertical eye position φ (up positive). Crosses (+) are attempted fixations; corresponding circles (○) are actual positions of the right eye; the deviation from normal torsion (given by Eq. [1]) is shown by the tilt of an arrow from upright, multiplied by five for visibility. (A) Patient data. (B) Simulation: eye with denervated SO. (C) Simulation: result of further manual and automatic eye parameter manipulations (see text).

circles are the actual positions of the abnormal, following right eye. Where torsional data were collected, the deviation from normal torsion (as given by Listing's law) is shown as the tilt of an arrow from the upright, multiplied by 5 for visibility.

The patient's preoperative Hess chart shows that: (1) when the left eye is fixing primary position (point *a* in Fig. 10A) the right eye is 5° above primary position (*a'*). (2) For all positions in which the left eye is looking down (point *b* or *c*, for example), the right eye (*b'*, *c'*) is 7°–12° too high. (3) The right eye shows too much adduction (compare, say, the horizontal offset of *a* and *a'*),

and this problem tends to become worse as the eyes look down. Finally, (4) there is considerable extorsion, especially in down gaze (point c'). This patient was troubled by diplopia, especially when she tried to read. She had no stereopsis.

The obvious start for simulating this abnormality is simply to denervate the right SO. This is done by setting $\lambda_d[SO] = 0$ in Table I and so in Eqs. [7]. The muscle will still exert a force on the globe by virtue of its passive elasticity (Eq. [6] with $F_d = 0$); it simply is no longer affected by innervation. Since we suppose the patient's left eye to be normal, the procedure of Fig. 9E is used to generate each point in a model Hess chart. The result is shown in Fig. 10B.

With only the right SO denervated the model shows: (1) an elevation of primary position, but less than that of the patient; (2) a defect of depression, but only when the eye is in adduction; depression in abduction is much better than that of the patient; (3) some tendency to adduct in depression, but less than that of the patient; (4) a pattern of extorsion very much like that of the patient.

The model tells us, then, that we are on the right track, but that the patient has further complications. We have assumed that the original trauma only denervated the right SO, and a review of the clinical records does not suggest otherwise. Any additional pathology must be a consequence of the paralysis. We note that several months passed between the bicycle accident and Scott's examination. During that time, the right SO probably underwent some atrophy; we guess that this might be reflected by reducing λ_p. Further, it is well known that an innervated muscle that operates in a habitually shortened state tends to develop a contracture, or increase in its passive stiffness. Compared to a normal right eye, our patient's eye is, on average, elevated and adducted. We suspect, then, that the passive forces of muscles which shorten in elevation (SR and IO) and in adduction (MR) will increase. The muscles these pull against (their *antagonists*) might become somewhat "stretched," reducing their passive force.

These considerations allow a more refined preoperative simulation. In addition to $\lambda_d[SO] = 0$, we set $\lambda_p[SO] = 0.31$, (25% less than 0.41, Table I) and invoke the parameter searching program with $\lambda_p[LR]$, $\sigma_p[LR]$, $\lambda_p[MR]$, $\sigma_p[MR]$, $\lambda_p[SR]$, $\sigma_p[SR]$, $\lambda_p[IR]$, $\sigma_p[IR]$, $\lambda_p[IO]$, $\sigma_p[IO]$ as the parameters to be searched.

The parameter searching program suggests small changes in the stiffnesses of the horizontal recti, decreasing that of the LR ($\lambda_p[LR]$ from 1.00 to 0.75, and $\sigma_p[LR]$ from 1.00 to 0.82), and increasing that of the MR ($\lambda_p[MR]$ from 1.07 to 1.32 and $\sigma_p[MR]$ from 1.00 to 1.16). As we expected there are increases in the stiffness (contractures) of the muscles that elevate the eye. ($\lambda_p[SR]$ from 0.80 to 1.84, $\lambda_p[IO]$ from 0.38 to 0.74, $\sigma_p[SR]$ from 1.00 to 1.16, and $\sigma_p[IO]$ from 1.00 to 1.30). Changes in the IR are negligible.

Figure 10C shows the Hess chart for this model eye: it is a good simulation of the main features of the clinical data: (1) the elevation of primary position, (2) the limitation of depression, (3) the excess adduction in depression, and (4) the extorsion shown by the patient are all well matched by the simulation. There is a discrepancy, however, in that the simulation shows depression to be worse in

adduction. This is due to the actions of the oblique muscles; their vertical actions are greater in adduction than abduction so the loss of the SO is more noticeable in adduction. This is the usual finding in SO palsy, and our model persists in reflecting it. Its absence in this particular patient is unusual and suggests some mechanical or innervational variation in her eye mechanics, which we did not explore further.

To treat this case, Scott did surgery on both eyes. He recessed the left IR 4.5 mm, and recessed the right IO to a point 11 mm from the limbus (the border separating the iris and sclera) and 2.5 mm from the lateral border of the IR. It was expected that this would lower the right eye relative to the left eye, especially on leftward gaze. A partial (9/10) tenotomy was performed on the right MR, through its upper edge near the insertion. By thus lowering its effective insertion, the action of the MR in downgaze was weakened, reducing the tendency of the eye to adduct in this position. The two recessions were modeled by appropriate movements of the insertions. The MR tenotomy was modeled as a 30° bending of the insertion ($B_0[MR] = -30.0$) and a 2-mm recession.

Note that surgery was on both eyes so that, now, neither eye is normal. Thus, we must use the full binocular simulation shown in Fig. 9.

The patient's postsurgical chart is shown in Fig. 11A and the model's prediction of surgical outcome is shown in Fig. 11B. The prediction is quite good: (1) There is a good match for primary position; (2) depression is improved in both the actual and simulated charts; (3) adduction in depression is reduced in both, however, (4) the model does not, make a good prediction of extorsion in downgaze. Note that, the need to improve alignment in depression (so that the patient could read comfortably) resulted in a misalignment in elevation and that the simulation predicts this.

In summary; (1) we achieved a reasonable preoperative simulation in which the parameter searching program made some plausible suggestions; (2) there was a good prediction of surgical outcome, and (3) we could have predicted that a deficit in elevation would result from the surgery. This latter would not

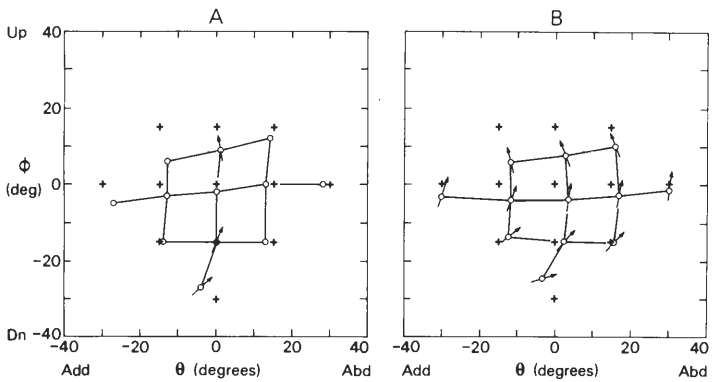

FIG. 11. Postoperative Hess charts. (A) Patient data. (B) Simulation (see text).

necessarily lead us to suggest different surgery, since good alignment in downgaze was the primary goal of surgery, and no surgery could correct all positions of gaze.

At their present stage of development, our surgical simulations are quite accurate in some cases, but less impressive in others. Our hope is that, with further refinement and testing, we will be able to both improve the model and better define the class of strabismic disorders about which it makes the best predictions.

12. Implementation

The SQUINT simulation system is organized around three commands (operators) and the three types of data files they output (see Fig. 12). The commands all run as independent UNIX processes (there is no SQUINT executive) so that the UNIX facilities for I/O redirection and job control may be used. The files are all ASCII strings, allowing full use of UNIX text manipulation programs.

The three types of files are: (1) Innervation files, each line of which has a value of *iv* for each of the six muscles of an eye. (2) Eye position files, each line of which has the three coordinates of an eye position (ϑ, φ, ψ). (3) Eye parameter files, which give the mechanical and innervational parameters of an eye. Table I, for instance, gives the parameters of a normal eye.

The three corresponding commands are: (1) "inn," which reads an eye parameter file and an eye position file, and finds the innervation sets which would drive the specified eye to the specified positions. (2) "pos," which finds the

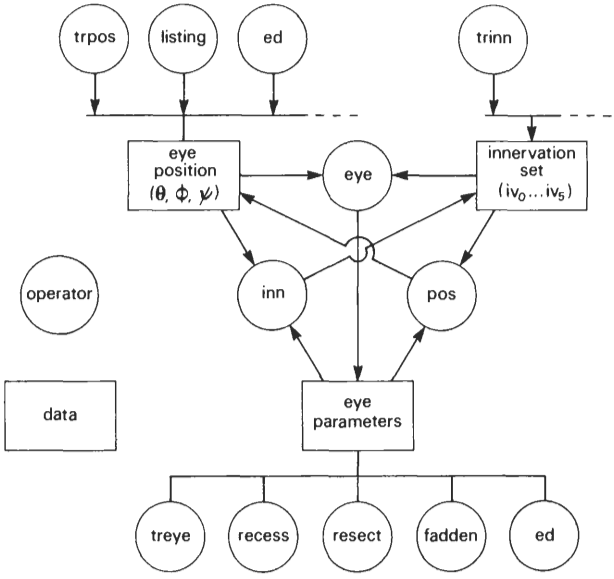

FIG. 12. SQUINT operators and data files (see text).

positions the specified eye would go to under the specified innervations. (3) "eye" (the automatic parameter searching program), which tries to characterize an eye that would move to the specified positions under the specified innervations.

There are also commands which operate on a single file type, producing a file of the same type. The surgery commands (recess, resect, faden), for instance, operate on eye parameter files, yielding modified eye parameter files that reflect the effects of surgery. Any text editor, such as "ed," can also be used to modify eye parameter files. Pretty-print programs "trpos," "trinn," and "treye" trim down the precision and otherwise prepare eye position, innervation, and eye parameter files for human viewing. Creating a new eye position file is most easily done with an editor. Normal values of ψ can then be entered in the file with "listing" (which computes Eq. [1]). "Intrp" (see "Binocularity" above and Fig. 9A) is a bit different in that it operates on two eye position files (one describes the $\psi(\vartheta, \varphi)$ surface, and the other gives the desired ϑ and φ values).

Compound commands allow more complex simulations; they are actually UNIX Shell scripts composed of simple commands. "hc1" and "hc2," for instance, stimulate the monocular and binocular Hess tests by performing the sequences of operations shown in Fig. 9 for the desired array of fixations. These commands produce both tabular and graphical output, the latter being compatible with UNIX "plot" filters.

In designing the SQUINT system we sought to make it portable, modifiable, and, of course, correct.

Extensive portability was achieved by choosing UNIX as the operating system. Most of the code is written in C and has passed the "lint" error-checking compiler. A few programs are written in ANSI Fortran, so that a Fortran 77 compiler is also required. Since its development on a Digital Equipment PDP-11/45 running a mixture of JHU UNIX (from Johns Hopkins University) and Version 7 UNIX (Bell Laboratory), it has been ported to a Digital Equipment VAX-11/780 under 4.2 BSD UNIX (University of California, Berkeley), and to a Masscomp MC-500 under RTU System III UNIX (Masscomp).

The system will certainly be modified as more is learned about orbital mechanics and innervation. To facilitate changes we have made SQUINT highly modular at both the command and subroutine levels. Care has been taken to make the source code easy to read. Each source file contains informative headers and comments. Debugging code is included in the source files and may be optionally compiled.

The SQUINT source code occupies about 0.4 Mbytes. About 2.0 Mbytes is enough disc space for the entire system including the source, object library, load modules, and some user-produced output. Several SQUINT processes are larger than 64 kbytes; machines (such as small PDP-11s) with limited addressing range may be unable to run the full system.

We are pleased to make SQUINT available for research purposes to any interested investigator.

ACKNOWLEDGMENTS

This research was supported by Grants EY00598, EY07047, and EY04565 from the National Eye Institute, National Institute of Health, Bethesda, Maryland. Computations were performed on computer facilities at the Wilmer Institute, supported by Core Facility Grant EY01765, and at the Smith–Kettlewell Institute, supported by the Smith–Kettlewell Eye Research Foundation and Grant BRSG S07 RR05566-19 from the Biomedical Research Support Grant Program, National Institutes of Health.

REFERENCES

1. ROBINSON, D. A. A quantitative analysis of extraocular muscle cooperation and squint. *Invest. Ophthalmol.* **14,** 801 (1975).
2. NAKAYAMA, K. Coordination of extraocular muscles. *In* "Basic Mechanisms of Ocular Motility and Their Clinical Implications" (G. Lennerstrand and P. Bach-y-Rita, Eds.), pp. 193–207. Pergamon, New York, 1975.
3. SHERRINGTON, C. S. Experimental note on two movements of the eye. *J. Physiol. (London)* **17,** 27 (1894).
4. VOLKMANN, A. W. On the mechanics of the eye muscles. *Ber. Verh. K. Saechs. Ges. Wiss.* **21,** 28 (1869).
5. NAKAGAWA, T. Topographic anatomical studies on the orbit and its contents. *Acta Soc. Ophthalmol. Japan.* **69,** 2155 (1965).
6. VON NOORDEN, G. K. "Binocular Vision and Ocular Motility: Theory and Management of Strabismus," 2nd ed. Mosby, St. Louis, Mo., 1980.
7. "Vision Research: A National Plan 1983–1987: The 1983 Report of The National Advisory Eye Council," Vol. 1, p. 43. USDHHS, PHS, NIH, 1983.
8. ROBINSON, D. A., O'MEARA, D. M., SCOTT, A. B., *et al.* Mechanical components of human eye movements. *J. Appl. Physiol.* **26,** 548 (1969).
9. COLLINS, C. C., SCOTT, A. B., AND O'MEARA, D. M. Elements of the peripheral oculomotor apparatus. *Amer. J. Optom.* **46**(7), 510 (1969).
10. KERNIGHAN, B. W. AND RITCHIE, D. M. "The C Programming Language." Prentice–Hall, Englewood Cliffs, N.J., 1978.
11. COLLINS, C. C., CARLSON, M. R., SCOTT, A. B., AND JAMPOLSKY, A. Extraocular muscle forces in normal human subjects. *Invest. Ophthalmol. Visual Sci.* **20**(5), 652 (1981).
12. COLLINS, C. C. The human oculomotor control system. *In* "Basic Mechanisms of Ocular Motility and Their Clinical Implications" (G. Lennerstrand and P. Bach-y-Rita, Eds.), pp. 145–180. Pergamon, New York, 1975.
13. KREWSON, W. E. The action of the extraocular muscles; A method of vector analysis with computations. *Trans. Amer. Ophthalmol. Soc.* **48,** 443 (1950).
14. BOEDER, P. Co-operative action of extraocular muscles. *Brit. J. Ophthalmol.* **46,** 397 (1962).
15. JUDGE, S. J., RICHMOND, B. J., AND CHU, F. C. Implantation of magnetic search coils for measurement of eye position: An improved method. *Vision Res.* **20,** 535 (1980).
16. FRANCE, T. D., AND BURBANK, D. P. Clinical applications of a computer-assisted eye model. *Trans. Amer. Acad. Ophthalmol. Otolaryng.* **86,** 1407 (1979).
17. HOTCHKISS, M. G., MILLER, N. R., CLARK, A. W., AND GREEN, W. R. Bilateral Duane's Retraction Syndrome: A clinical–pathological case report. *Arch. Ophthalmol.* **98,** 870 (1980).
18. DYER, J. A., AND HENDERSON, J. W. Orbitonometry in unilateral exophthalmos. *Amer. J. Ophthalmol.* **45,** 208 (1958).
19. AKIMA, H. A method of bivariate interpolation and smooth surface fitting for irregularly distributed data points. *ACM Trans. Math. Software.* **4**(2), 148 (1978).